J|A|C|S ARTICLES

Published on Web 06/22/2010

Explanation of the Adsorption of Polar Vapors in the Highly Flexible Metal Organic Framework MIL-53(Cr)

Sandrine Bourrelly,[†] Béatrice Moulin,[‡] Angel Rivera,[§] Guillaume Maurin,[*,§] Sabine Devautour-Vinot,[§] Christian Serre,[||] Thomas Devic,[||] Patricia Horcajada,[||] Alexandre Vimont,[*,‡] Guillaume Clet,[‡] Marco Daturi,[‡] Jean-Claude Lavalley,[‡] Sandra Loera-Serna,[†] Renaud Denoyel,[†] Philip L. Llewellyn,[†] and Gérard Férey[||]

Laboratoire Chimie Provence, UMR 6264, Universités Aix-Marseille I, II & III—CNRS, Centre de Saint Jérôme, 13397 Marseille cedex 20, France, Laboratoire Catalyse et Spectrochimie, UMR CNRS 6506, ENSICAEN and Université de Caen, 6 boulevard du Maréchal Juin, 14050 Caen cedex, France, Institut Charles Gerhardt Montpellier, UMR CNRS 5253, UM2, ENSCM, Place E. Bataillon, 34095 Montpellier cedex 05, France, and Institut Lavoisier, UMR CNRS 8180, Université de Versailles Saint-Quentin-en-Yvelines, 45 avenue des Etats-Unis, 78035 Versailles cedex, France

Received March 19, 2010; E-mail: alexandre.vimont@ensicaen.fr; guillaume.maurin@univ-montp2.fr

Abstract: A comparison of the adsorption of water, methanol, and ethanol polar vapors by the flexible porous chromium(III) terephthalate MIL-53(Cr) was investigated by complementary techniques including adsorption gravimetry, *ex situ* X-ray powder diffraction, microcalorimetry, thermal analysis, IR spectroscopy, and molecular modeling. The breathing steps observed during adsorption strongly depend on the nature of the vapor. With water, a significant contraction of the framework is observed. For the alcohols, the initial contraction is followed by an expansion of the framework. A combination of IR analysis, X-ray diffraction, and computer modeling leads to the molecular localization of the guest molecules and to the identification of the specific guest−guest and host−guest interactions. The enthalpies of adsorption, measured by microcalorimetry, show that the strength of the interactions decreases from ethanol to water. Differential scanning calorimetry experiments on an EtOH/H_2O mixture suggest a selective adsorption of ethanol over water.

Introduction

Alcohols are attractive candidates as renewable, environmentally friendly sources of energy. Among them, the bioalcohols ethanol and methanol can be used as fuels via their conversion to gasoline ("methanol-to-gasoline" or "methanol-to-olefins" processes).[1,2] In some processes, water acts as a contaminant which may reduce the conversion by competitive occupation of active sites.[3] In order to circumvent this problem, adsorption by porous materials can provide an efficient method of purification, due to their easy regeneration under relatively mild conditions. Hybrid porous solids, either rigid or flexible (see refs 4−9 and references therein), have already proved to be very promising for gas/vapor storage, due to their very large pore volumes and their low cost of desorption.[10–19]

Using these porous hybrids, we and others have studied adsorption of vapors[20−25] including long-chain hydrocarbons, alcohols, and water. The corresponding solids sometimes exhibit

[†] Universités Aix-Marseille I, II & III.
[‡] ENSICAEN and Université de Caen.
[§] UM2.
[||] Université de Versailles Saint-Quentin-en-Yvelines.

(1) Keil, F. J. *Microporous Mesoporous Mater.* **1999**, *29*, 49–66.
(2) Stocker, M. *Microporous Mesoporous Mater.* **1999**, *29*, 3–48.
(3) Moller, K. P.; Bohringer, W.; Schnitzler, A. E.; van Steen, E.; O'Connor, C. T. *Microporous Mesoporous Mater.* **1999**, *29*, 127–144.
(4) Férey, G. *Chem. Soc. Rev.* **2008**, *37*, 191–214.
(5) Kitaura, R.; Fujimoto, K.; Noro, S.; Kondo, M.; Kitagawa, S. *Angew. Chem., Int. Ed.* **2002**, *41*, 133–135.
(6) Férey, G.; Serre, C. *Chem. Soc. Rev.* **2009**, *38*, 1380–1399.
(7) Fletcher, A. J.; Thomas, K. M.; Rosseinsky, M. J. *J. Solid State Chem.* **2005**, *178*, 2491–2510.
(8) Kitagawa, S.; Uemura, K. *Chem. Soc. Rev.* **2005**, *34*, 109–119.
(9) Uemura, K.; Matsuda, R.; Kitagawa, S. *J. Solid State Chem.* **2005**, *178*, 2420–2429.
(10) Murray, L. J.; Dinca, M.; Long, J. R. *Chem. Soc. Rev.* **2009**, *38*, 1294–1314.
(11) Latroche, M.; Surblé, S.; Serre, C.; Mellot-Draznieks, C.; Llewellyn, P. L.; Lee, J. H.; Chang, J. S.; Jhung, S. H.; Férey, G. *Angew. Chem., Int. Ed.* **2006**, *45*, 8227–8231.
(12) Li, Y.; Yang, R. T. *Langmuir* **2007**, *23*, 12937–12944.
(13) Millward, A. R.; Yaghi, O. M. *J. Am. Chem. Soc.* **2005**, *127*, 17998–17999.
(14) Llewellyn, P. L.; Bourrelly, S.; Serre, C.; Vimont, A.; Daturi, M.; Hamon, L.; De Weireld, G.; Chang, J. S.; Hong, D. Y.; Hwang, Y. K.; Jhung, S. H.; Férey, G. *Langmuir* **2008**, *24*, 7245–7250.
(15) Kondo, M.; Yoshitomi, T.; Seki, K.; Matsuzaka, H.; Kitagawa, S. *Angew. Chem., Int. Ed. Engl.* **1997**, *36*, 1725–1727.
(16) Eddaoudi, M.; Kim, J.; Rosi, N.; Vodak, D.; Wachter, J.; O'Keeffe, M.; Yaghi, O. M. *Science* **2002**, *295*, 469–472.
(17) Seki, K.; Mori, W. *J. Phys. Chem. B* **2002**, *106*, 1380–1385.
(18) Llewellyn, P. L.; Maurin, G.; Devic, T.; Loera-Serna, S.; Rosenbach, N.; Serre, C.; Bourrelly, S.; Horcajada, P.; Filinchuk, Y.; Férey, G. *J. Am. Chem. Soc.* **2008**, *130*, 12808–12814.
(19) Llewellyn, P. L.; Horcajada, P.; Maurin, G.; Devic, T.; Rosenbach, N.; Bourrelly, S.; Serre, C.; Vincent, D.; Loera-Serna, S.; Filinchuk, Y.; Férey, G. *J. Am. Chem. Soc.* **2009**, *131*, 13002–13008.
(20) Eddaoudi, M.; Li, H. L.; Yaghi, O. M. *J. Am. Chem. Soc.* **2000**, *122*, 1391–1397.
(21) Lee, J. Y.; Olson, D. H.; Pan, L.; Emge, T. J.; Li, J. *Adv. Funct. Mater.* **2007**, *17*, 1255–1262.
(22) Trung, T. K.; Trens, P.; Tanchoux, N.; Bourrelly, S.; Llewellyn, P. L.; Loera-Serna, S.; Serre, C.; Loiseau, T.; Fajula, F.; Férey, G. *J. Am. Chem. Soc.* **2008**, *130*, 16926–16932.

 10.1021/ja1023282

Scheme 1. Structural Switching Evolution of the MIL-53(Cr) Solid upon Adsorption of Some Gases[36]

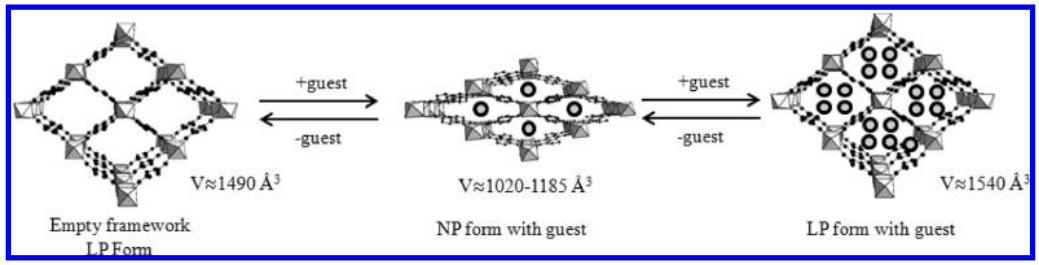

selective properties: either an affinity for water[26,27] over organic solvent or alcohols or a preferential adsorption of organic solvents or alcohols[28] over water.[29] When water is adsorbed, an initial nonwetting or hydrophobic character can be noticed prior to any significant uptake.[30,31] However, until now, these various behaviors have been observed but rarely clearly explained. An approach to understanding such phenomena requires the involvement of complementary techniques able to provide convergent structural, spectroscopic, and thermodynamic information at the atomic scale. That is the primary aim of this paper.

Moreover, to conduct such an analysis, the choice of the solid is crucial. It must provide significant and easily measurable effects during adsorption/desorption in order to ensure accurate data from which the explanation of adsorption phenomena will be extracted. For this reason, we selected the flexible porous structure type MIL-53 (M = Al, Cr, Fe, Ga),[32−35] represented here by chromium(III) terephthalate (or MIL-53(Cr), MIL standing for Materials of Institut Lavoisier). Its cell volume varies by close to 40% between the large-pore (LP) and the narrow-pore (NP) forms (Scheme 1) during adsorption/desorption of several gases when sufficient interactions of these gases with the pore wall of this solid are present.[18]

The so-called "breathing effect" of the hybrid flexible solids is now recognized[5,6] and presents two main aspects: (i) nonporous-to-porous transitions (gate opening[37,38] and interwoven solids[39,40]) and (ii) structural transitions between various porous phases, which can occur in one or several steps.[41,42]

The present paper concerns the study of the adsorption mechanisms of pure water and alcohol (methanol, ethanol) vapors in MIL-53(Cr) solid, using the results of the following complementary techniques: (i) adsorption/desorption gravimetry experiments as well as a newly developed controlled desorption experiment, (ii) *ex situ* X-ray powder diffraction (XRD) and *in situ* infrared (IR) spectroscopy for the analysis of the host−guest interactions, and (iii) adsorption calorimetry and differential scanning calorimetry (DSC) for providing the energetics of adsorption and their application to separation studies. Finally, the excellent agreement between these experimental data and those we extracted from computer modeling confirms the validity of such an approach to successfully characterize the complex adsorption behavior of flexible hybrid materials.

The paper is presented in three parts. The first one deals with the experimental details, and the second part describes the investigation of the solid behavior during the whole adsorption process. The third part focuses on the desorption process and preliminary information on the water−alcohol selectivity.

Experimental Section

Synthesis. MIL-53(Cr) was synthesized using the published procedure,[33] while an alternative activation method was performed in two steps: (i) exchange of the free terephthalic acid molecules filling the pores with DMF at 150 °C overnight, and (ii) evacuation of DMF upon calcination at 250 °C under air atmosphere overnight.[36a] This procedure eliminates most of the residual organic fragments in the pores of the structure.

Vapor Properties. The investigated solvents were water, methanol, and ethanol. The liquids were distilled, and the alcohols were further stored over a drying agent (zeolite 5A) prior to use. Some of their characteristics are listed in Table 1.

Adsorption and Desorption Isotherms. The adsorption isotherms were obtained by gravimetry. The laboratory-made adsorption apparatus includes a symmetrical balance and allows a continuous introduction of vapor to the sample in a slow enough manner to ensure quasi-equilibrium between the vapor and solid and a high-resolution isotherm plot.[43] For each series of experiments, this quasi-equilibrium condition is verified by stopping the

(23) Finsy, V.; Kirschhock, C. E. A.; Vedts, G.; Maes, M.; Alaerts, L.; De Vos, D. E.; Baron, G. V.; Denayer, J. F. M. *Chem.—Eur. J.* **2009**, *15*, 7724–7731.
(24) Maji, T. K.; Uemura, K.; Chang, H. C.; Matsuda, R.; Kitagawa, S. *Angew. Chem., Int. Ed.* **2004**, *43*, 3269–3272.
(25) Fletcher, A. J.; Cussen, E. J.; Prior, T. J.; Rosseinsky, M. J.; Kepert, C. J.; Thomas, K. M. *J. Am. Chem. Soc.* **2001**, *123*, 10001–10011.
(26) Gu, J. Z.; Lu, W. G.; Jiang, L.; Zhou, H. C.; Lu, T. B. *Inorg. Chem.* **2007**, *46*, 5835–5837.
(27) Chen, B. L.; Ji, Y. Y.; Xue, M.; Fronczek, F. R.; Hurtado, E. J.; Mondal, J. U.; Liang, C. D.; Dai, S. *Inorg. Chem.* **2008**, *47*, 5543–5545.
(28) Zhang, J. P.; Chen, X. M. *J. Am. Chem. Soc.* **2008**, *130*, 6010–6017.
(29) Pan, L.; Parker, B.; Huang, X. Y.; Olson, D. H.; Lee, J.; Li, J. *J. Am. Chem. Soc.* **2006**, *128*, 4180–4181.
(30) Kusgens, P.; Rose, M.; Senkovska, I.; Frode, H.; Henschel, A.; Siegle, S.; Kaskel, S. *Microporous Mesoporous Mater.* **2009**, *120*, 325–330.
(31) Horike, S.; Tanaka, D.; Nakagawa, K.; Kitagawa, S. *Chem. Commun.* **2007**, 3395–3397.
(32) Loiseau, T.; Serre, C.; Huguenard, C.; Fink, G.; Taulelle, F.; Henry, M.; Bataille, T.; Férey, G. *Chem.—Eur. J.* **2004**, *10*, 1373–1382.
(33) Serre, C.; Millange, F.; Thouvenot, C.; Noguës, M.; Marsolier, G.; Louër, D.; Férey, G. *J. Am. Chem. Soc.* **2002**, *124*, 13519–13526.
(34) Whitfield, T. R.; Wang, X. Q.; Liu, L. M.; Jacobson, A. J. *J. Solid State Sci.* **2005**, *7*, 1096–1103.
(35) Volkringer, C.; Loiseau, T.; Guillou, N.; Férey, G.; Elkaim, E.; Vimont, A. *Dalton Trans.* **2009**, 2241–2249.
(36) (a) Serre, C.; Bourrelly, S.; Vimont, A.; Ramsahye, N. A.; Maurin, G.; Llewellyn, P. L.; Daturi, M.; Filinchuk, Y.; Leynaud, O.; Barnes, P.; Férey, G. *Adv. Mater.* **2007**, *19*, 2246–2251. (b) Salles, F.; Ghoufi, A.; Maurin, G.; Bell, R. G.; Mellot-Draznieks, C.; Férey, G. *Angew. Chem., Int. Ed.* **2008**, *47*, 8487.
(37) Kitaura, R.; Seki, K.; Akiyama, G.; Kitagawa, S. *Angew. Chem., Int. Ed.* **2003**, *42*, 428.
(38) Maji, T. K.; Mostafa, G.; Matsuda, R.; Kitagawa, S. *J. Am. Chem. Soc.* **2005**, *127*, 17152–17153.
(39) Biradha, K.; Hongo, Y.; Fujita, M. *Angew. Chem., Int. Ed.* **2002**, *41*, 3395–3398.
(40) Seki, K. *Phys. Chem. Chem. Phys.* **2002**, *4*, 1968–1971.
(41) Choi, H. J.; Dinca, M.; Long, J. R. *J. Am. Chem. Soc.* **2008**, *130*, 7848.
(42) Matsuda, R.; Kitaura, R.; Kitagawa, S.; Kubota, Y.; Belosludov, R. V.; Kobayashi, T. C.; Sakamoto, H.; Chiba, T.; Takata, M.; Kawazoe, Y.; Mita, Y. *Nature* **2005**, *436*, 238–241.
(43) Rouquérol, J.; Davy, L. *Thermochim. Acta* **1978**, *24*, 391–397.

Table 1. Several Properties of the Investigated Polar Vapors

	H_2O	CH_3OH	C_2H_5OH
boiling temperature, T_b (K)[46]	373.15	337.69	351.80
liquid molar volume at 298 K, V_{liq} ($cm^3 \cdot mol^{-1}$)[46]	18.07	40.73	58.68
enthalpy of vaporization at 298 K, $\Delta_{vap}h$ ($kJ \cdot mol^{-1}$)[46]	40.66	35.21	38.56
molecular dipole moment, μ (D)[46]	1.8	1.7	1.7
saturation vapor pressure at 298 K, $p°$ (Torr)[47]	24	119	58

vapor introduction and ensuring that no change in pressure or mass is observed. A typical adsorption−desorption isotherm takes around 10 days. To carefully measure the desorption of the water vapor from the fully hydrated MIL-53(Cr), a new experimental procedure was used,[44] in which the porous solid is initially immersed in an excess of liquid and then slowly evacuated under controlled vacuum conditions (through a capillary toward vacuum).

Adsorption Microcalorimetry. Gravimetry is the method most suited to determine the adsorption isotherm of vapor, but it is difficult to combine it with a microcalorimeter. Therefore, direct measurements of adsorption energies have been performed using a Tian-Calvet microcalorimeter coupled to a laboratory-made volumetric device, allowing a point-by-point procedure or a continuous introduction of vapor.[45] A syringe pump is used to inject and vaporize the liquid inside the calorimetric cell. For this study, the injection of liquid has been performed in a stepwise manner.

For both adsorption experiments, ca. 40 mg of sample is used. Prior to the measurements, the sample is outgassed at 523 K for 12 h under vacuum ($\sim 10^{-2}$ mbar).

X-ray Powder Diffraction. To determine the structure of the NP forms of MIL-53(Cr) in the presence of water and the two alcohols, high-resolution XRD patterns were collected at 298 K using powdered samples prepared *ex situ*. The powder was introduced in glass capillaries and outgassed overnight at 523 K prior to introduction of vapor at room temperature; it was then equilibrated at a given partial pressure (water, methanol, or ethanol) using a laboratory-made vapor introduction system and finally flame-sealed. The corresponding diffractograms were recorded at the Swiss-Norwegian Beamlines at the European Synchrotron Radiation Facility using a MAR345 imaging plate at a sample-to-detector distance of 250 mm, $\lambda = 0.69402$ Å. The data were integrated using the Fit2D program (Dr. A. Hammersley, ESRF) and a calibration measurement of a NIST LaB_6 standard sample. The resulting powder patterns were indexed in monoclinic cells (see Table 2, below) using the Dicvol software.[48] The atomic coordinates of the NP MIL-53 framework were used as a starting model, and refinement using Fullprof and its graphical interface Winplotr[49,50] Fourier difference maps (SHELXL/SHELXTL software[51,52]) allowed the location of water or alcohol molecules within the pores of MIL-53. Refinement provided a good agreement with the experimental data. For the crystallographic details, see Table S1 and Figures S1−S3 in the Supporting Information.

Infrared Spectroscopy. IR spectra were recorded with a Nicolet FT-IR spectrometer. Samples were deposited on a silicon wafer and activated at 473 K under a vacuum (open form). Increasing vapor pressures were introduced successively in the IR cell. At 300 K, for each pressure, spectra were taken until equilibrium was reached, i.e., when no additional modification was observed.

The amount of adsorbed gas was determined by the integrated area of characteristic peaks ($\delta(H_2O)$ for water, ν(CH) massif for methanol and ethanol). The coverage was estimated by the decrease of the hydroxyl signals (δ(OH) band at ca. 920 cm^{-1}) relative to the initial bands. The fraction of the open form was estimated by the relative intensity at 1022 or 596 cm^{-1} compared to the initial spectra after activation.[36]

Differential Scanning Calorimetry. The energetic features of the solvent desorption from MIL-53(Cr) were studied by DSC with a Netzsch DSC 204F apparatus under a nitrogen atmosphere, with a heating rate of 2 $K \cdot min^{-1}$ in the temperature range 173−433 K. Prior to the DSC measurements, the samples were dehydrated at 473 K under a vacuum and then brought into contact with an atmosphere of saturated vapor of the selected solvent for 24 h at 295 K. This saturation was performed in a glovebag under an argon atmosphere, in order to prevent any contamination from air.

Molecular Modeling. The initial atomic coordinates of the hybrid MIL-53(Cr) porous framework in the absence/presence of polar vapors were taken directly from the refined structure obtained by XRD. Since the positions of the H atoms cannot be detected by such experimental techniques, these atoms were added to the organic groups and to the μ_2 position, using the H-adding function in the Accelrys Materials Studio Visualizer software.[53] For the organic part, this means that hydrogen atoms were added to the six-membered aromatic rings, keeping consistent with well-established C−H bond lengths (1.14 Å) and C−C−H bond angles (120°). For the inorganic part, the hydrogen atoms were included such that the O−H bonds were completely perpendicular to the M−O−M linkages, and the bond lengths were set at 0.95 Å. The starting possible adsorption arrangements for water, methanol, and ethanol in the pores of MIL-53(Cr) were generated by chemical intuition. Energetically favorable formation of a hydrogen bond can be expected between the polar part of the vapor molecule and the μ_2-OH group present at the MIL-53(Cr) surface. Thus, using this information, different starting configurations of possible arrangements corresponding to one and two vapor molecules per pore of MIL-53(Cr) were built in order to (i) be consistent with the experimental content explored by *ex situ* XRD and (ii) provide an estimation of the interaction energy for the different vapor molecules. Optimization of the various configurations for a given vapor molecule content always resulted in the same geometry. Geometry optimization of all these structures was then performed using periodic density functional theory calculations with the PW91 GGA density functional[54] and the double numerical basis set containing polarization functions on hydrogen atoms (DNP),[55] as implemented in the DMol^3 code. It has already been revealed that the PW91 functional performs well to describe the hydrogen-bonded systems.[56,57] The interaction energy between MIL-53(Cr) and the polar molecule was obtained as the difference between the energy of the DFT-optimized structures containing one vapor molecule per pore and the energy sum of the DFT-optimized single constituents.[58] We did not correct our energies for basis set

(44) Denoyel, R.; Barrande, M.; Beurroies, I. Characterisation of porous solids from nanometer to micrometer range by capillary condensation. In *7th International Symposium on the Characterization of Porous Solids (COPS-VII)*, Aix-en-Provence, France, 2007;Elsevier: Amsterdam, 2007.
(45) Denoyel, R.; Beurroies, I.; Vincent, D. *J. Therm. Anal.* **2002**, *70*, 483–492.
(46) Poling, B. E.; Prausnitz, J. M.; O'Connell, J. P. *The properties of gases and liquids*, 5th ed.; McGraw-Hill: New-York, 2001.
(47) Lide, R. D. *CRC Handbook of Chemistry and Physics*, 83rd ed.; CRC Press: Boca Raton, FL, 2003.
(48) Boultif, A.; Louër, D. *J. Appl. Crystallogr.* **1991**, *24*, 987–993.
(49) Rodriguez-Carvajal, J. *Collected Abstracts of Powder Diffraction Meeting*, Toulouse, France, 1990.
(50) Roisnel, T.; Rodriguez-Carvajal, J. *Abstracts of the 7th European Powder Diffraction Conference*, Barcelona, Spain, 2000.
(51) *SHELXL-97*; University of Göttingen: Göttingen, Germany, 1997.
(52) Sheldrick, G. M. *Acta. Crystallogr.* **2008**, *A64*, 112−122.
(53) *Materials Studio Visualiser*; Accelrys Inc.: San Diego, CA, 2005.
(54) Perdew, J. P.; Wang, Y. *Phys. Rev. B* **1992**, *45*, 13244–13249.
(55) Hehre, W. J.; Ditchfield, R.; Pople, J. A. *J. Chem. Phys.* **1972**, *56*.
(56) Gale, J. D. A density functional study of molecular adsorption in zeolites *Conference on Recent Advances in the Study and Preparation of Novel Surfaces*, in Honour of the Award of the Centenary Medal of the UK-RSC to Prof. K. I. Zamaraev, London, England, Jan 26, 1995; Baltzer Sci Publ Bv.:London, 1995.
(57) Tsuzuki, S.; Lüthi, H. P. *J. Chem. Phys.* **2002**, *114* (9), .

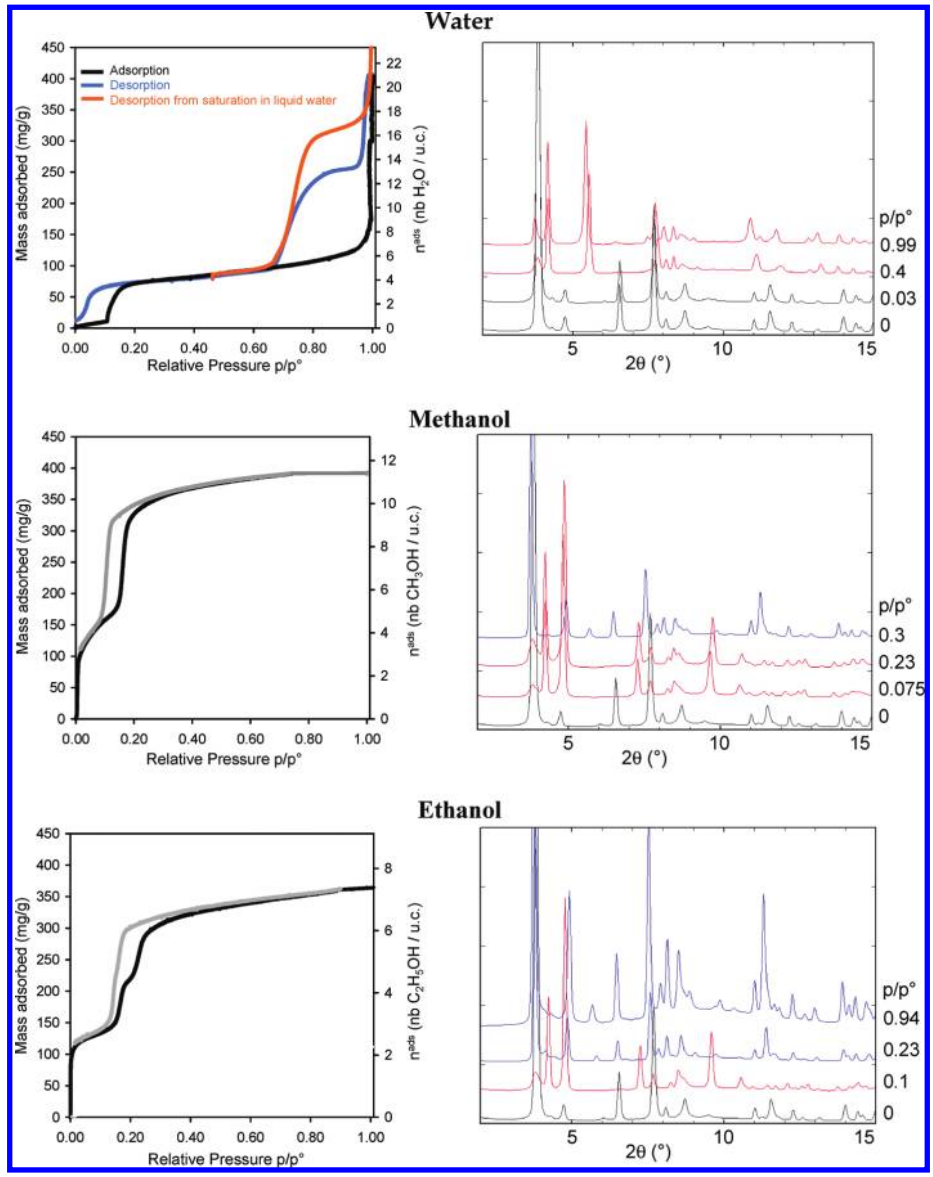

Figure 1. Left: Adsorption (black line) and desorption (gray line) isotherms of vapors as a function of the relative pressure at 298 K. Right: *Ex situ* X-ray powder diffraction patterns of MIL-53(Cr) at 298 K. Three different partial pressures of vapors have been used: black/blue and red colors represent the LP and NP forms of MIL-53(Cr), respectively. In the case of water: adsorption (black curve) and desorption (blue curve) isotherms of water vapor as a function of the relative pressure at 298 K obtained by gravimetry. A second desorption isotherm, the orange curve, has been obtained from the solid saturated in water excess (controlled desorption experiment). In all the cases, stepwise hysteretic adsorption and desorption are observed. Their position strongly depends on the nature of the guest molecules.

superposition error (BSSE) effects,[60] as the Dmol^3 code uses exact DFT spherical atomic orbitals.

Results and Discussion

1. General Aspects: Isotherms and Structures. Adsorption−desorption isotherms on MIL-53(Cr) have been measured by gravimetric methods using a continuous introduction of vapors at 25 °C (Figure 1). The rather small initial adsorption of water below $p/p° = 0.1$ indicates relatively weak interactions and suggests some "hydrophobic" character of the MIL-53(Cr) present initially in its LP form, as already observed for other MILs (MIL-101(Cr) and MIL-100(Fe)[30]). Above this relative pressure, the adsorption increases before reaching a plateau at $p/p° = 0.9$. Toward saturation, the uptake again sharply increases in a pressure range where liquefaction occurs.

The shape of the adsorption isotherms of the two alcohols differs drastically from that of water. Indeed, the initial adsorption is immediate. The sharp increase in the range $0 < p/p° < 0.05$ is followed first by a plateau and then by a second filling around $p/p° \geq 0.2$. The latter occurs in one (methanol) or two (ethanol) steps. In contrast to water, no important alcohol uptake is observed near the saturation pressures.

The adsorption/desorption process was also followed by IR spectroscopy. For water, integrating the area of the characteristic peak ($\delta(H_2O)$) at 1626 cm^{-1} at different relative pressures provides an estimate of the amount of adsorbed water. A similar procedure was applied for the adsorption of methanol and ethanol considering the ν(CH) massif. The resulting "optical"

(58) Delley, B. *J. Chem. Phys.* **1990**, *92*, 508–517.

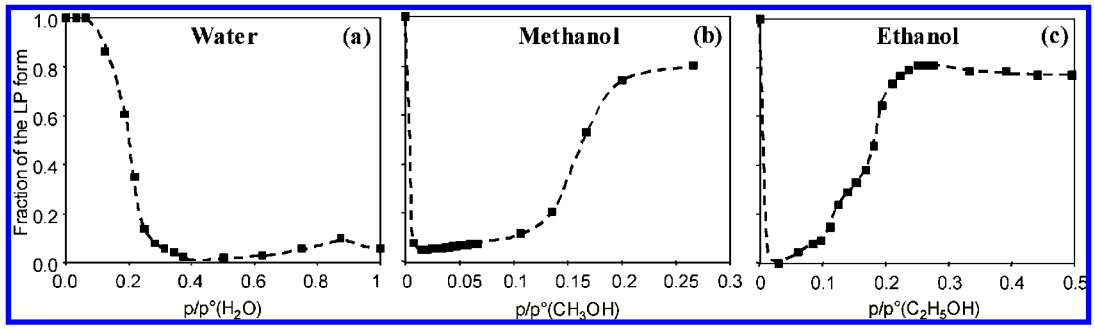

Figure 2. Fraction of the LP form upon (a) water, (b) methanol, or (c) ethanol adsorption estimated by following the intensity of the band at 1022 (water and ethanol) and 596 cm^{-1} (methanol) as a function of the relative pressure.

Table 2. Cell Parameters of MIL-53(Cr) at Different Stages of Pore Opening in the Presence of Polar Vapors

	a (Å)	*b* (Å)	*c* (Å)	*β* (deg)	*V* (Å^3)	*p*/*p*°	space group
dried MIL-53(Cr)	16.73(1)	13.03(1)	6.81(1)		1486(1)	0	*Imcm*
H_2O	19.64(1)	9.23(1)	6.81(1)	107.6(1)	1017(1)	0.4	*C2/c*
CH_3OH	19.64(1)	9.15(1)	6.81(1)	107.2(1)	1168(1)	0.075	*C2/c*
C_2H_5OH	19.62(1)	9.30(1)	6.81(1)	107.4(1)	1185(1)	0.10	*C2/c*
CH_3OH	16.13(1)	13.96(1)	6.83(1)		1538(1)	0.30	*Imcm*
C_2H_5OH	16.15(1)	13.97(1)	6.83(1)		1541(1)	0.94	*Imcm*

isotherms (Figures S4 and S5, Supporting Information) nicely fit with those obtained by gravimetry.

At this stage, *ex situ* synchrotron XRD patterns were collected (Figure 1) at different partial vapor pressures in a first step to correlate the macroscopic and molecular aspects of the adsorption phenomenon. These data were compared with *in situ* IR spectroscopy measurements at different partial vapor pressures (Figure 2 and Figure S6, Supporting Information).

The XRD patterns clearly show that the activated solid, prior to any adsorption, corresponds to the LP form of the MIL-53(Cr) solid. The introduction of vapors first transforms it into the contracted NP form (Table 2). In all cases, the isotherm plateaus correspond to saturation of the available porosity, whatever the NP or LP forms. In their NP forms, the unit cell volumes of the MIL-53(Cr)−guest system are 1017, 1168, and 1185 Å^3 for water, methanol, and ethanol, respectively (Table 2). The NP form thus adapts its pore size to the size of the entrapped species, i.e., the van der Waals volumes, as already observed for other guests. On the other hand, the volumes of the LP forms in the presence of the alcohols are identical and close to those previously reported for the dried or C_2H_6-rich MIL-53(Cr) forms (>1535 Å^3).[18]

Beside these structural data for the host framework, IR spectroscopy can provide some additional information.[36] The evolution with pressure of the intensities of the bands at 1022 (structural band ν_{18a}) or 596 cm^{-1} (ν(Cr−O)), normalized to their original ones in activated MIL-53(Cr), allows access to the fraction of the LP form as a function of $p/p°$ (Figure 2). These quantitative results are consistent with the evolution of the XRD patterns when one increases the concentration of the various vapors as well as the shape of the isotherms reported in Figure 1.

For water, the adsorption step around $p/p° = 0.1$ corresponds to a region where the LP structure starts to contract and transform into the NP phase. Above $p/p° = 0.1$ and up to 0.25, the fraction of the LP form decreases sharply and then more gradually between 0.25 and 0.4. Above $p/p° = 0.4$, and in agreement with XRD (see Figure 1), the LP form is no longer present. One can note that, above $p/p° = 0.6$, the slight increase of the fraction of the LP form may indicate a partial swelling of the structure, as already observed during CO_2 adsorption.[36] Both XRD and IR experiments confirm the difficulty of reopening the MIL-53(Cr) with water vapor (48 h at $p/p° \approx 1$), even though such a transformation occurs in the liquid phase after 24 h. This suggests that kinetic effects intervene. Nevertheless, as will be seen below, the full pore opening does occur in liquid water to reach the required 17 molecules per unit cell. The situation is completely different with alcohols (Figures 1 and 2b,c). The NP form of MIL-53(Cr) appears as soon as the vapors are in contact with the dry solid. The shrinkage is complete at very low relative pressures. For both alcohols, a gradual reopening of the porosity to the LP form then appears for pressures between $p/p° = 0.1$ and 0.3 (Figure 2). Above $p/p° = 0.3$, the fraction of the LP form reaches 80%.

This contrast between the behaviors of water and the alcohols clearly indicates the influence of the nature of the vapor on the breathing conditions. Whereas only the LP→NP transition exists for water, the successive sequence LP→NP→LP is observed for alcohols. Nevertheless, while this is just an observation, an explanation of this behavior is required which calls for further experiments to obtain thermodynamic (with microcalorimetry and DSC), spectroscopic (*in situ* IR), and structural information at the molecular level to deepen our understanding of the phenomenon and the various microscopic mechanisms in play. Molecular modeling was also developed for the energetic and structural aspects to compare experience and simulation. The conclusions will be reported in two parts related respectively to the LP→NP transition when the adsorption starts and to the second NP→LP transition during the reopening.

2. Initial Adsorption and LP→NP Transition. Before detailing the results, some supplementary but important information on the MIL-53 structure type (Scheme 1) must be recalled. One of the characteristics of this topology is the existence of chains of octahedra linked by corners, these corners corresponding to OH groups. In terms of metal coordination, the presence of octahedra indicates that the metallic sites are coordinatively saturated and cannot be identified as adsorption sites; only OH groups of the skeleton (hereafter noted OH_{sk}) can be identified as such. Moreover, previous IR studies using CH_3CN as a

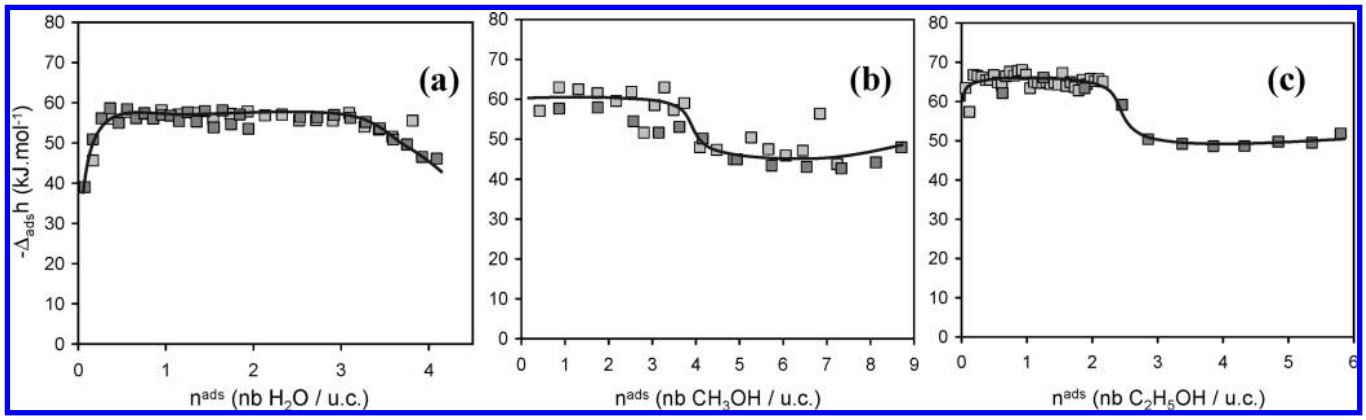

Figure 3. Differential adsorption enthalpies of water (a), methanol (b), and ethanol (c) as a function of the number of vapor molecules adsorbed per unit cell. The reported data were collected from two experiments. Lines are to guide the eyes.

probe[59] have shown acidic character of the OH_{sk} groups ($\Delta\nu(OH_{sk}) = 180$ cm^{-1}), their strength being close to that of phenol.[60] The oxygen of the OH_{sk} is slightly basic, as revealed by the adsorption of CO_2.[59] These features are important to consider prior to any discussion on the interactions. Several types of interactions can already be envisaged: (i) OH_{sk}−guest, (ii) organics of the skeleton−guest, and (iii) guest−guest. The results below will try to elucidate their respective contributions.

In terms of the interaction energy, microcalorimetry evaluates the extent of the various interactions that occur during adsorption. The differential adsorption enthalpies, measured for water and alcohols up to $p/p° \approx 0.25$, are shown in Figure 3 as a function of the number of molecules per unit cell (u.c.). For water, the initial interactions, up to 0.2 mol·u.c.$^{-1}$, are slightly below its enthalpy of liquefaction (−40.66 kJ·mol^{-1}, Table 1). They confirm the initial relatively "hydrophobic" nature of the LP form of MIL-53(Cr), illustrated by the low uptake of water at low pressure. In agreement, the IR spectrum obtained under a low water pressure ($p/p° = 0.06$, Figure 4) reveals that only a small amount of OH_{sk} in LP form acts as adsorption sites; their characteristic bands (3653 (ν(OH)) and 928 cm^{-1} (δ(OH)) are shifted to 3380 and 1035 cm^{-1}, respectively, indicating the formation of a hydrogen-bonding complex between OH_{sk} and H_2O for which the OH_{sk} group is proton donor.

Above an adsorption of 0.2 water molecule per unit cell, the enthalpies increase up to a relatively constant value of around −57 kJ·mol^{-1}, close to the values already observed for other MOFs.[21,61−63] This increase corresponds to the abrupt step in the isotherm at $p/p° = 0.1$ when the NP structural form starts to appear. This would correspond to the onset of strong water−host interactions. Indeed, such a strong interaction is confirmed by IR spectroscopy: further water addition shifts upward the position of the perturbed δ(OH) vibration of OH_{sk} groups from 1035 to 1065 cm^{-1} (Figure 4). The energy profile starts to decrease above 3 H_2O/u.c., tending toward the saturation capacity corresponding to the plateau (4 H_2O/u.c.). This might

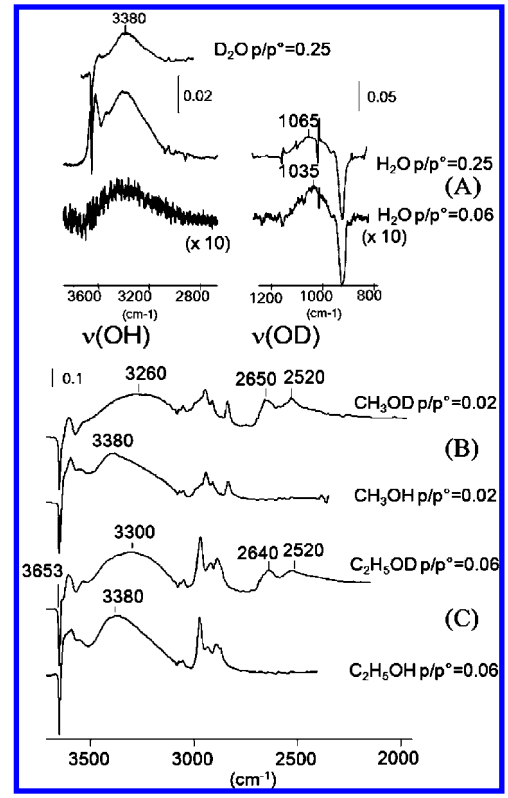

Figure 4. IR spectra of MIL-53(Cr) after introduction of vapor at low $p/p°$ and comparison with the deuterated vapors. The LP fractions are 100% and 13% at $p/p° = 0.06$ and 0.25, respectively, for water (A), 5% for methanol (B), and 1.5% for ethanol (C).

indicate the increasing contribution of vapor−vapor interactions which are less energetic than those of the host−guest interactions and announce the transition to the more open LP form.

Microcalorimetric measurements show that the curves for methanol and ethanol adsorption have similar shapes (Figure 3b,c). They show two domains within which the enthalpies are almost constant. The step change observed for each alcohol corresponds to the saturation capacity of the NP form, as evoked above (4 guest molecules/u.c.). Low amounts adsorbed correspond to the adsorption by NP, while the largest adsorbed amounts correspond to the LP form. The enthalpies of adsorption in the NP form (∼ −60 and −65 kJ·mol^{-1} for methanol and ethanol, respectively) are larger than in the case of water (−57 kJ·mol^{-1}). Therefore, the host−guest interactions are stronger in the case of alcohols than for water. This observation is in

(59) Vimont, A.; Travert, A.; Bazin, P.; Lavalley, J. C.; Daturi, M.; Serre, C.; Férey, G.; Bourrelly, S.; Llewellyn, P. L. *Chem. Commun.* **2007**, 3291–3293.
(60) Purcell, K. F.; Drago, R. S. *J. Am. Chem. Soc.* **1967**, *89*, 2874–2879.
(61) Cheng, L.; Lin, J. B.; Gong, J. Z.; Sun, A. P.; Ye, B. H.; Chen, X. M. *Cryst. Growth Des.* **2006**, *6*, 2739–2746.
(62) Lin, X.; Blake, A. J.; Wilson, C.; Sun, X. Z.; Champness, N. R.; George, M. W.; Hubberstey, P.; Mokaya, R.; Schroder, M. *J. Am. Chem. Soc.* **2006**, *128*, 10745–10753.
(63) Kondo, A.; Daimaru, T.; Noguchi, H.; Ohba, T.; Kaneko, K.; Kanob, H. *J. Colloid Interface Sci.* **2007**, *314*, 422–426.

Scheme 2. Alcohol Interactions with the Structural Cr−OH Groups (R = CH_3 or CH_3CH_2)

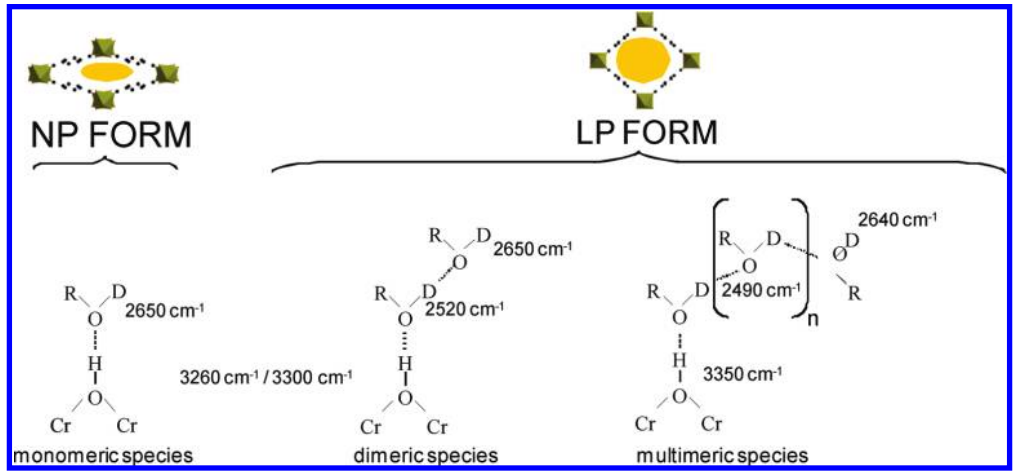

agreement with the following IR observations. Indeed, the IR results relative to alcohol adsorption show that, in contrast to water adsorption, the first molecules significantly perturb the OH_{sk} (Figure 4 and Figures S8 and S9, Supporting Information) and rapidly transform the structure to the NP form (Figure 2), in agreement with XRD and gravimetric measurements (Figure 1). The extent of the $\nu(OH_{sk})$ shift ($\Delta\nu(OH_{sk})$) has been measured using deuterated alcohols and D_2O (Figure 4). It is equal to 270 (3653 − 3380), 390 (3653 − 3260), and 350 cm^{-1} (3653 − 3300) for water, methanol, and ethanol, respectively. It represents the strength of hydrogen-bonding between the OH_{sk} group and the guest molecule, which is significantly lower for water.

However, the sequence ($\Delta h^{ads}_{EtOH} > \Delta h^{ads}_{MeOH} > \Delta h^{ads}_{HOH}$) is different from that deduced from the $\Delta\nu(OH_{sk})$ shift (MeOH > EtOH> HOH). This shows that the strength of the hydrogen-bonding between the OH_{sk} group and the guest molecule is not the only interaction to take into account. Alkyl groups also certainly play a role. Indeed, the range of differences between EtOH and MeOH values (~5 kJ·mol^{-1}), already pointed out by Li *et al.* for another hybrid material (~6.3 kJ·mol^{-1}),[21] reflects the energy contribution of the additional CH_2 group.

Which interactions are involved in such enthalpies? We have already noted the importance of OH_{sk} groups in this context. Even for small amounts of introduced guests, IR spectroscopy (Figure 4) can indicate, on a local basis, which hydroxyl groups are affected.

Following the adsorption of deuterated alcohols (R−OD) by IR spectroscopy helps to determine the nature of the species formed, since the ν(OD) frequency around 2650 cm^{-1} is quite different from that of OH_{sk} (3653 cm^{-1}), which allows one to discriminate between the OH_{sk} and the hydroxyls groups of the guest.

The results collected in Figure 4 unambiguously show two bands corresponding to the ν(OD) vibration of the ROD species. They are situated near 2650 and 2520 cm^{-1} for a low $p/p°$ value (Figure 4), revealing the presence of two types of adsorbed alcohols. Two assumptions can be put forward:

(i) Two types of monomeric species are formed, the alcohol hydroxyl group interacting either strongly (2520 cm^{-1} band) or weakly (2650 cm^{-1} band) with the surface. This hypothesis assumes the presence of heterogeneous basic sites (carboxylate groups, π electrons).

(ii) Monomeric and dimeric species are formed, the latter being characterized by the ν(OD) band at 2520 cm^{-1}, the terminal −OD group giving rise to the 2650 cm^{-1} band, whatever the species formed (Scheme 2). Such a scheme supposes the formation of dimeric species although in a limited amount since the two ν(OD) bands have the same intensity, whereas the molar absorption coefficient of the 2520 cm^{-1} band must be higher than that of the 2650 cm^{-1} one.[64] Four OH_{sk} groups per unit cell are expected, and 4 alcohol molecules/u.c. adsorb at the first plateau ($p/p° = 0.1$), which lead to one alcohol molecule per Cr−OH group. The DFT and XRD results reported below (Figure 5) do not support a strong interaction between two alcohol molecules adsorbed on two different Cr−OH groups in the NP form. However, we can consider that even for a low $p/p°$ ratio, a small fraction of the material presents a LP form which allows the formation of dimeric alcohol species. The IR range characteristic of the structural form (1015−1025 cm^{-1}) supports such an assumption: the 1019 cm^{-1} band shifts slightly toward higher wavenumbers when the ethanol $p/p°$ ratio increases from 0.05 to 0.1 (see subtracted spectrum, Figure S7, Supporting Information). It is worth noticing that the 2650 cm^{-1} band characterizing the terminal ROD group is located below the expected value for an OD group free of any interaction (2690 cm^{-1}). It could indicate weak interactions between the hydroxyl group of alcohol and an H-acceptor center such as the O atoms of carboxylate moieties, π electrons of the terephthalic groups, or the oxygen of the Cr−OH group.

How are the guest molecules arranged to give rise to these interactions? This aspect was achieved by coupling molecular simulations with *ex situ* XRD refinements, more particularly when one reaches the plateau in the isotherm, i.e., for a relative pressure of 0.4, 0.075, and 0.1 for water, methanol, and ethanol, respectively. This corresponds in each case to 4 guest molecules/u.c. (Figure S10, Supporting Information).

From the positions of the water molecule refined from the XRD data (Figure 5 left), two types of host framework/guest interactions are present: (i) hydrogen bonds between the protons of the μ_2-OH_{sk} group of the skeleton and the oxygen atoms of the adsorbed water O_w, with a characteristic distance of 2.59(1) Å between the two oxygens (red arrows), and (ii) hydrogen bonds between the protons of O_w molecules and the oxygen atoms of the carboxylate present in the upper and lower chains of MIL-53(Cr) [distances: 3.13(1) and 3.42(1) Å, respectively (blue arrows)]. In addition, the water O_w molecules in the tunnels form strong hydrogen bonds between each other. Further DFT

(64) Burneau, A.; Corset, J. *Can. J. Chem.* **1974**, *52*, 915–923.

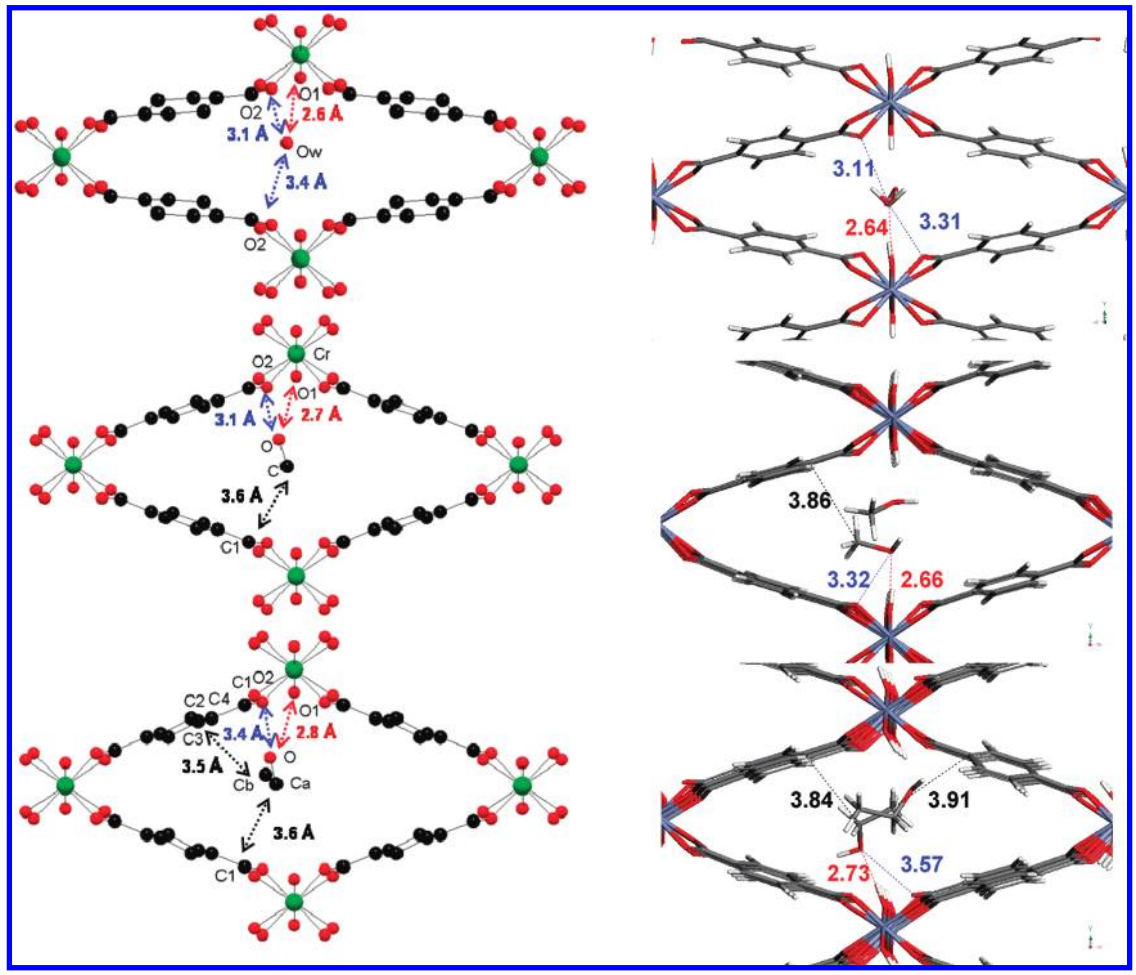

Figure 5. Left: XRD crystal structure of the guest molecules in the NP MIL-53(Cr) forms (top to bottom: water, methanol, ethanol). The pore opening of the narrow pores forms MIL-53_guest (guest: water, methanol, ethanol) increases as expected with the size of the guest molecules from ~1017 Å^3 for the water form up to ~1185 Å^3 for the ethanol form. Chromium, oxygen, and carbon atoms are shown in green, red, and black, respectively. For a better understanding, atoms involved in the host−guest interactions have been shown. Right: DFT-optimized geometries (top to the bottom: water, methanol, ethanol) in the NP form for a loading of 2 vapor molecules per pore of MIL-53(Cr) (4 polar molecules/u.c.). Cr, O, C, and H atoms are labeled in purple, red, gray, and white, respectively. The distances are reported in angstroms.

calculations (Figure 5 right) nicely confirm the experimental refinement (simulated values: 2.64, 3.11, and 3.31 Å, respectively). They clearly show that the water molecules are arranged in a strong hydrogen bond network (O···H distance 1.92 Å). These additional interactions could explain why the $\Delta\nu(OH_{sk})$ value does not reflect the $O_{sk}-O_{guest}$distance.

Such highly ordered arrangements of molecules along the tunnel, as previously observed for CO_2,[36] lead to guest−guest interactions that would contribute to the existence of the MIL-53 framework in its NP form. Furthermore, by optimizing the structure corresponding to 1 H_2O/u.c. (Figure S11, Supporting Information), it was also possible to estimate the interaction energy between the water molecule and the framework to be −49.7 kJ·mol^{-1}, which is consistent with the microcalorimetry data (−57 kJ·mol^{-1}).

Alcohols present both common and different features with the case of water. Here, three types of host−guest interactions are shown (Figure 5): (i) The hydrogen bonds are still present between the protons of the OH_{sk} groups (chains) and the oxygen atoms (O_{ol}) of the guests. The $O_{sk}\cdots O_w$ distances (2.70(1) Å for methanol, 2.80(1) Å for ethanol, shown in red in Figure 5) are longer than for water (2.60 Å). (ii) In contrast to water, hydrogen bonds exist between the protons of the guest molecules and the oxygen atoms of the carboxylates (shown in blue in Figure 5). While water interacts with the lower and upper chains, the alcohols only interact with one chain at a time, with a slightly stronger interaction for methanol compared to ethanol (3.14(1) vs 3.36(1) Å). (iii) In addition to the interactions observed in water, there are van der Waals interactions between the alkyl groups of alcohols and the aromatic rings of the framework. Once again, the behaviors of methanol and ethanol are slightly different, with the $-CH_3$ groups of methanol interacting with only one chain at a time while the $-CH_2$ and $-CH_3$ groups of a single ethanol molecule interact with two different chains at a time.

DFT-optimized structures for the same vapor loading confirm the existence of three types of interactions pointed out by the structural refinements. Simulations also emphasize the existence of additional interactions between the alkyl group and the organic spacer of MIL-53(Cr). In addition, by optimizing the structure corresponding to a single methanol and single ethanol molecule per pore (Figure S11), interaction energies for both methanol and ethanol have been estimated to be −50.6 and −55.4 kJ·mol^{-1}, respectively. This simulated energetic trend (ethanol > methanol > water) is consistent with that obtained experimentally by microcalorimetry.

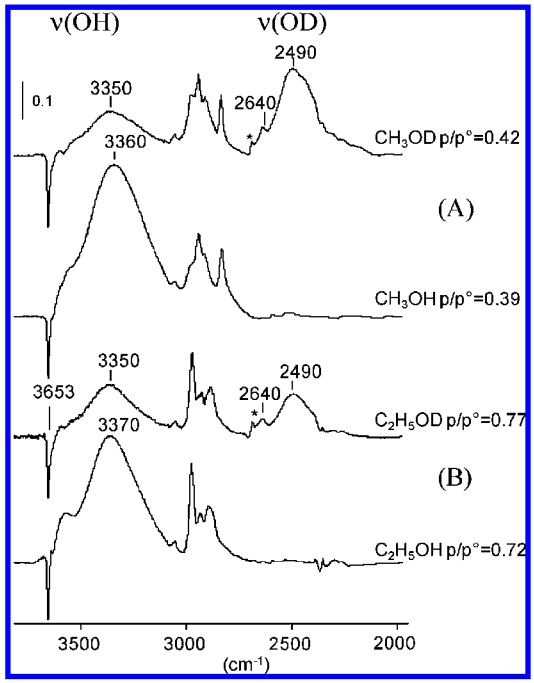

Figure 6. IR spectra of MIL-53(Cr) after introduction of alcohol at higher loadings and comparison with the deuterated vapors: (A) methanol 76% LP and (B) ethanol 75% LP.

3. NP→LP Transition: Adsorption in the LP Form and Desorption. The NP→LP transition only exists for alcohols, and the progressive reopening of the structure occurs before reaching the saturation vapor pressure. At high alcohol loadings, the ν(OH) band of the perturbed OH_{sk} is situated at 3350 cm^{-1} (Figure 6), e.g., at a higher wavenumber than that observed in the NP form (3260/3300 cm^{-1}). This indicates that the strength of the hydrogen bond between OH_{sk} and alcohols is weaker in the LP form. The strong and broad ν(OD) band situated at 2490 cm^{-1} reveals that the hydroxyl group of the alcohols are engaged in hydrogen bonds resulting from the formation of multimeric species (Scheme 2); the terminal hydroxyl group of the chain gives rise to a weak ν(OD) band at 2640 cm^{-1}, a wavenumber close to that reported for alcohols in the NP form. This indicates that the hydroxyl groups of the terminal molecule are weakly hydrogen-bonded to framework basic centers.

Besides van der Waals associations, the size of the guest molecules can also justify the easy reopening of MIL-53(Cr) in the case of alcohols. Keeping in mind that the most contracted form of the MIL-53 topology occurs for MIL-53(Fe), with a cell volume of ca. 900 $Å^3$,[65] hosting guest molecules increases it in the NP form (1017.7 $Å^3$ for water and close to 1170 $Å^3$ for alcohols).The higher value in the latter case would make the NP→LP transition easier, as less initial contraction occurs. Incidentally, by impregnation in liquid alcohols, one can unambiguously reach the saturation capacity of the LP form in the MIL-53(Cr) system. It decreases from methanol (~12 CH_3OH/u.c.) to ethanol (~8 C_2H_5OH/u.c.) following the increase of the size of the polar molecule.

One can note that, in the case of *vapors*, this behavior is associated with two structural transitions corresponding to contraction and swelling, which is quite unusual except for the "jungle-gym" solid.[66] Indeed, in general, flexible MOF materials induce only one kind of structural change during the adsorption (expansion, contraction, or distortion). However, for the MIL-53 solid, this two-step adsorption mechanism during the breathing process was already observed for a number of *gaseous* probe molecules (CO_2 and hydrocarbons).

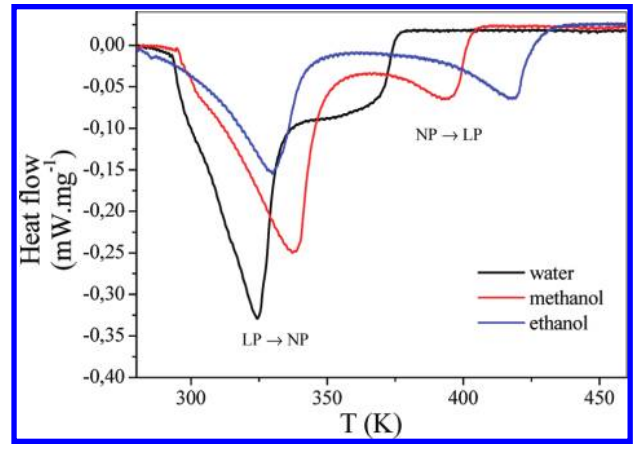

Figure 7. DSC plots of the MIL-53(Cr) previously brought into contact with a vapor of pure water (black line), methanol (red line), and ethanol (blue line).

For water, the origin of the sharp increase of the included amount at $p/p° \approx 1.0$ could be associated with condensation of water in the experimental device; however, one cannot eliminate the possibility that part of the water molecules can also be adsorbed by the sample at this point. A further analysis of this could be provided by the desorption experiments.

In all cases, desorption isotherms show hysteresis. In the case of water, the horizontal part of the desorption, measured directly after the adsorption (Figure 1, blue curve), reveals the remaining water adsorbed at the saturation vapor pressure. This amount of water (about 255 $mg \cdot g^{-1}$), corresponding to 13 H_2O/u.c., confirms that the adsorption process continues at relative pressures close to 1. Nevertheless, the desorption isotherm depends strongly on at which point the final increase in adsorption is reached, indicating that kinetic effects intervene. As a variation of the desorption curve was noted around $p/p° = 1$, which can be related to our experimental conditions (saturation time), and as full saturation of the LP structure is not reached, a second experiment was carried out to better follow the desorption process from $p/p° = 1$ to 0.45. This controlled desorption experiment was developed recently,[44] in which the sample is initially oversaturated with the liquid before desorption under well-controlled conditions. It can be seen on the resulting curve (in orange) that the optimal saturation of the porosity is around 17 H_2O/u.c. (value taken from the horizontal part of curve C for $0.85 < p/p° < 0.95$), which is closer to the value of ~26 H_2O/u.c. estimated from the porous volume of the LP form of MIL-53(Cr) (~0.50 $cm^3 \cdot g^{-1}$), although the experimental pore opening of MIL-53(Cr) saturated with water vapor is still unknown.

To gain further information about the differences in desorption behavior in MIL-53(Cr) for all three vapors, complementary DSC measurements have been performed in an appropriate range of temperature (Figure 7). DSC signals were obtained for the samples equilibrated with an atmosphere of saturated vapor of

(65) Millange, F.; Guillou, N.; Walton, R. I.; Greneche, J. M.; Margiolaki, I.; Ferey, G. *Chem. Commun.* **2008**, 4732–4734.

(66) Uemura, K.; Yamasaki, Y.; Komagawa, Y.; Tanaka, K.; Kita, H. *Angew. Chem., Int. Ed.* **2007**, *46*, 6662–6665.

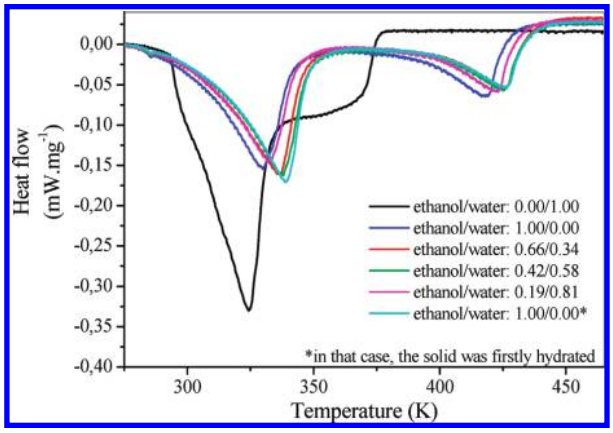

Figure 8. DSC plots of the MIL-53(Cr) previously brought in contact with a vapor mixture of ethanol/water, whose molar composition of the gaseous phase is 0.66/0.34 (red line), 0.42/0.58 (green line), or 0.19/0.81 (magenta line), compared to the ones obtained for the desorption of pure water (black line) and pure ethanol (blue line). The DSC signal of the hydrated MIL-53(Cr) brought in contact with a pure vapor of ethanol is also shown (cyan line).

the selected solvent for 24 h at 295 K, to ensure that the solid is in its LP form, consistent with observation from the desorption branch of the isotherms (Figure 1). One can notice that the signals exhibit a complex profile. They can be decomposed into two contributions, which are both endothermic, suggesting that the desorption in MIL-53(Cr) follows two distinct steps from the initial solvated LP to the NP forms, and then from the NP to the anhydrous LP forms, respectively.[67]

While the first DSC endothermic peak appears in the same domain of temperatures for the three polar molecules, the second one corresponds to the desorption of the molecules from the NP form. It is shifted toward higher temperatures for the desorption of alcohols compared to that for water. The shift is more pronounced for ethanol than for methanol. This confirms that the strength of interactions follows the sequence water < methanol < ethanol, as previously observed by microcalorimetry, IR, and molecular simulations. Furthermore, for alcohols, particularly for ethanol, the second peak appears in a temperature range for which the DSC signal for water is no longer significant. This behavior would suggest that a separation starting from a vapor mixture could be expected.

For a preliminary validation of this assumption, DSC experiments were performed to follow the desorption features of the MIL-53(Cr) sample, initially brought in contact with different ethanol/water vapor mixture atmospheres (see details in the Supporting Information). As shown in Figure 8, the DSC signals are similar to those previously observed in the case of desorption of pure ethanol. As these experiments do not show any departure of water from the sample, it might suggest that only ethanol from the vapor mixture was initially adsorbed in MIL-53(Cr). Such an assumption is also supported by the fact that the resulting TGA signals of the MIL-53(Cr) solvated in the same conditions are similar in terms of weight loss and profile to those obtained for pure ethanol desorption (Figures S12 and S13, Supporting Information). Moreover, the IR spectrum of MIL-53(Cr) recorded under an EtOH/water vapor mixture at the saturation state does not reveal any significant band characteristic of adsorbed water, whereas a band for adsorbed EtOH is clearly observed (Figure S14, Supporting Information). The MIL-53(Cr) solid is thus expected to only adsorb ethanol from the mixture up to the saturation state, consistent with a higher affinity for ethanol compared to water as mentioned above on the basis of microcalorimetry and DFT calculations. In order to verify this assumption, we measured the DSC signal of MIL-53(Cr) first hydrated, i.e., kept in contact with the vapor of pure water for 10 days, and further solvated with a vapor of pure ethanol for 24 h. As shown in Figure 8, the similarity of these data to the DSC response of the solid solvated with pure ethanol vapor leads us to envisage that the ethanol molecules totally dispelled the initial adsorbed water out of the solid. To confirm this, the same sample was analyzed by TGA, in which the emanated vapors were analyzed using a mass analyzer (Figure S15, Supporting Information). It was shown that the signals attributed to water remain flat in the whole temperature domain, whereas those of ethanol are clearly detected for both steps of the desorption process, confirming that only ethanol is desorbed. This whole set of data would confirm that MIL-53(Cr) solid can be seen as a promising material for the selective adsorption of alcohols from alcohol/water vapor mixtures, in view of applications of alcohols purification.

Conclusion

The adsorption of polar vapors on MIL-53(Cr) lead to structural transitions: two for alcohols (methanol and ethanol), i.e., a partial closing and a reopening of the pores, whereas with water the framework was not able to switch to the large-pore open form in the vapor phase. We have observed experimentally the signature of this breathing effect with significant steps in the adsorption isotherms, with the structures determined by *ex situ* XRD for each step, and with IR spectroscopy from the variations of the structural band. We can note a common step for all these polar vapors, in which the structure is present in its narrow-pore form with 4 guest molecules per unit cell, and this corresponds to the occupancy of all the OH groups in a unit cell. Microcalorimetric measurements clearly show the different adsorption process, either in the NP form or in the LP form, and coupled with DFT calculations, it highlights that the adsorption of ethanol is more energetic than the adsorption of methanol and water. Two types of host framework/guest interactions are present for all the three polar vapors: (i) hydrogen bonds between the protons of the μ_2-OH group present at the surface of MIL-53(Cr) and the oxygen atoms of the guest molecule and (ii) hydrogen bonds between the protons of the guest molecules and the oxygen atoms of the carboxylate present in the chains of MIL-53(Cr). With one more alkyl group, a single ethanol molecule can interact with two different chains at one time (van der Waals interactions), whereas for methanol the interaction is possible only with one chain at a time. In addition, guest−guest interactions, absent in the case of alcohols but observed for water through the formation of a complex hydrogen-bonding network along the tunnel, contribute to the stabilization of the NP form of the hydrated MIL-53 by means of a strong "backbone" effect. This outcome supports our previous conclusions which emphasized that the presence of hydrogen-bonded OH groups plays a significant role in the stability of the NP form of the MIL-53.[68] Finally, a first

(67) Devautour-Vinot, S.; Maurin, G.; Henn, F.; Serre, C.; Devic, T.; Férey, G. *Chem Commun* **2009**, 2733–2735.

(68) Devic, T.; Horcajada, P.; Serre, C.; Salles, F.; Maurin, G.; Moulin, B. a.; Heurtaux, D.; Clet, G.; Vimont, A.; Grenèche, J.-M.; Ouay, B. L.; Moreau, F.; Magnier, E.; Filinchuk, Y.; Marrot, J. M.; Lavalley, J.-C.; Daturi, M.; Férey, G. *J. Am. Chem. Soc.* **2010**, *132*, 1127–1136.

experiment using a mixture of water and ethanol in the vapor phase suggests a possible selective adsorption of ethanol over water on the flexible MIL-53(Cr) solid.

Acknowledgment. The authors are indebted to CNRS, University of Versailles St Quentin, University of Montpellier 2, University de Provence, Ensicaen, and the French ANR (BLAN07-1_203677 SAFHS) for the funding and ESRF for providing Beamtime. We thank Martina Bejblova from J. Heyrovský Institute of Physical Chemistry (Czech Republic) and Yaroslav Filinchuk from ESRF for their help and fruitful discussions.

Supporting Information Available: Structural information and additional data obtained by IR spectroscopy, gravimetry, DFT, and thermal analysis. This material is available free of charge via the Internet at http://pubs.acs.org.

JA1023282